

Anatomical Heterogeneity in Transformer Language Models

Tomasz Wietrzykowski

Independent Researcher, Wrocław, Poland

March 12, 2026

Abstract

Current transformer language models are trained with uniform computational budgets across all layers, implicitly assuming layer homogeneity. In this work, we challenge this assumption through a comprehensive empirical analysis of SmoLLM2-135M - a 30-layer, 135M-parameter causal language model. We introduce a suite of diagnostic metrics including weight predictability (R^2), layer-wise ablation degradation, post-perturbation recovery speed, and weight manipulation robustness.

Our analysis reveals profound anatomical heterogeneity across six main findings: (1) Layer weights exhibit strong mathematical regularity ($R^2 = 0.91$ for MLP `gate_proj`) with a consistent oscillatory delta pattern (inter-layer delta correlation ≈ -0.50 for all components), yet simple regression-based weight generation fails catastrophically due to nonlinear error accumulation. (2) Layers form a distinct importance hierarchy ranging from a “critical core” (layers 8–11) where ablation causes up to +63,419% perplexity degradation, to redundant tissue, and - surprisingly - “anti-layers” (L14, L17) whose removal or perturbation *improves* model performance. (3) Recovery speed from perturbation strongly correlates with layer importance, suggesting differential training requirements per layer. (4) Among five tested weight manipulation strategies, only weight scaling ($\alpha = 0.9$) preserves generation quality (+49% PPL degradation vs. millions of percent for zeroing, cloning, or blending). (5) Based on these findings, we propose *Growth Transformer Training*, a paradigm that allocates training budget according to empirical layer importance and recovery dynamics. (6) A proof-of-concept experiment validates this strategy: a 12-layer heterogeneous Growth Transformer trained with six biological developmental phases achieves validation loss of 0.127 vs. 0.599 for a uniform baseline (4.7 \times improvement) in the same number of training steps and with identical parameter count, while being 13% faster.

These results suggest that transformer layers develop functional specialization analogous to biological organisms, and that embracing this heterogeneity during training yields substantial efficiency and quality gains.

Keywords: transformer architecture, layer importance, pruning, efficient training, weight manipulation, anti-layers, recovery speed, mechanistic interpretability

1. Introduction

1.1. Motivation

The transformer architecture [1] has become the standard for large language models (LLMs). Training protocols treat all layers uniformly: identical architectures, parameter budgets, and optimization steps. This uniformity implicitly assumes that all layers contribute equally to model function and require equivalent learning effort.

Biological neural systems, however, exhibit profound heterogeneity. Embryonic development proceeds in stages - notochord, neural tube, internal organs, surface structures - with radically different precision requirements per structure. We ask: do transformer layers exhibit an analogous importance hierarchy, and can this hierarchy be exploited to accelerate training?

1.2. Hypotheses

H1 (*Non-equivalence*) Transformer layers are not functionally interchangeable - ablating different layers causes radically different performance degradation.

H2 (*Predictability*) Later-layer weights are mathematically predictable from earlier weights, suggesting an internal “developmental pattern.”

H3 (*Differential trainability*) Layers differ in recovery speed after perturbation, correlating with importance and indicating heterogeneous training requirements.

H4 (*Anti-layers*) Certain layers may have a net-negative contribution - the model performs better with random weights in those layers than with trained weights.

1.3. Contributions

- First complete layer importance map of a small language model across all 30 layers with five independent metrics.
- Discovery of the *anti-layer phenomenon* - layers with net-negative contribution whose perturbation improves perplexity.
- Introduction of *Recovery Speed* as an empirical proxy for per-layer training budget requirements.
- Empirical evidence for a universal oscillatory weight-change pattern (delta correlation ≈ -0.50 across all components).
- Identification of the only effective weight manipulation strategy for redundant layers: weight scaling ($\alpha = 0.9$).
- *Growth Transformer Training*: a practical strategy achieving $\sim 54\%$ training cost reduction.

2. Related Work

2.1. Layer Analysis in Transformers

Tenney et al. [13] demonstrated that BERT layers encode different levels of linguistic information - lower layers capture syntax, upper layers semantics. Rogers et al. [10] confirmed hierarchical layer specialization in a comprehensive BERTology survey. These works focused on representational analysis rather than full weight-level importance quantification with manipulation experiments.

2.2. Pruning and Compression

Fan et al. [4] proposed LayerDrop - stochastic layer skipping during training to enable variable-depth inference. Sajjad et al. [11] analyzed layer dropping for efficiency. Michel et al. [8] showed that most attention heads are removable without significant degradation. Our approach differs in analyzing full-layer importance across multiple simultaneous metrics, and in revealing highly non-uniform, layer-specific importance profiles.

2.3. Efficient and Progressive Training

Gong et al. [5] proposed progressive stacking - gradually adding layers during training. Chen et al. [3] showed in EarlyBERT that earlier layers converge faster. Our work is complementary: rather than deciding when to add layers, we allocate *how much* training each layer requires, derived empirically from recovery speed measurements.

2.4. Weight Prediction and HyperNetworks

Ha et al. [6] proposed HyperNetworks - networks generating weights for other networks. Schurholt et al. [12] studied weight predictability across model zoos. Our finding of high R^2 (0.91) alongside catastrophic perplexity degradation from predicted weights reveals a critical nuance: statistical predictability of weights does not imply functional interchangeability.

3. Methodology

3.1. Model and Evaluation

We analyze SmoLLM2-135M [7], a decoder-only transformer with 30 layers, hidden dimension 576, 9 attention heads, and 135M total parameters. The primary metric is Perplexity (PPL) measured on a fixed held-out set of 10 diverse English sentences covering factual, definitional, and descriptive content. Baseline PPL = 22.60. The small model was chosen to enable hundreds of compute-intensive per-layer experiments without prohibitive GPU cost. Each layer contains 7 weight matrices: `q_proj`, `k_proj`, `v_proj`, `o_proj` (attention) and `gate_proj`, `up_proj`, `down_proj` (MLP).

3.2. Experiment 1: Layer Importance Map (Ablation)

For each layer $l \in \{0, \dots, 29\}$, we replace its weights with the average of its neighbors:

$$W_l \leftarrow \frac{W_{l-1} + W_{l+1}}{2}$$

and measure degradation $D_l = (\text{PPL}_l / \text{PPL}_{\text{baseline}} - 1) \times 100\%$. Classification thresholds: *Redundant* ($D < 10\%$), *Minor* ($10\% \leq D < 30\%$), *Important* ($30\% \leq D < 100\%$), *Critical* ($D \geq 100\%$). Negative D indicates improvement without trained weights - an anti-layer.

3.3. Experiment 2: Weight Predictability

For each component c and target layer $t \in \{2, \dots, 29\}$, we flatten weight matrices of layers $0 \dots t - 1$, subsample to 10,000 parameters, construct polynomial and sinusoidal features of layer indices $X = [l, l^2, \sin(l\pi/N), \cos(l\pi/N)]$, fit Ridge Regression, and report R^2 and cosine similarity of predicted vs. actual weights.

3.4. Experiment 3: Weight Structure Analysis

We compute the delta series $\Delta_l = W_{l+1} - W_l$ and measure Pearson correlation between consecutive deltas across all components. We also perform PCA on flattened weight matrices and compute pairwise cosine similarity between all layers.

3.5. Experiment 4: Weight Manipulation Strategies

We test five strategies for replacing weights in the 9 identified redundant layers simultaneously: (1) *Skip/Zero* - set weights to zero, relying on residual connections; (2) *Clone* - copy nearest non-redundant neighbor’s weights; (3) *Blend* - distance-weighted average of 4 nearest non-redundant neighbors; (4) *Low-rank blend* - SVD hybrid with directions from neighbor, magnitudes from original; (5) *Scale* - multiply original weights by $\alpha \in \{0.0, 0.1, 0.3, 0.5, 0.7, 0.9\}$.

3.6. Experiment 5: Recovery Speed

For each tested layer l , we inject Gaussian noise with $\sigma = 0.5 \times \text{std}(W_l)$, then freeze all layers except l and fine-tune using AdamW (lr = 10^{-4} , gradient clipping = 1.0). We record steps to reach PPL thresholds of $< 2\times$, $< 1.5\times$, and $< 1.1\times$ baseline. Tested layers: L0, L1, L3, L5, L8, L10, L11, L14, L17, L23, L24, L27, L29.

4. Results

4.1. Layer Importance Map

Table 1 presents the complete 30-layer ablation profile. The importance distribution spans from -0.6% to $+63,419\%$ - a range exceeding 10^7 .

Table 1: Complete layer importance profile for SmolLM2-135M. (*) Anti-layer: model achieves equal or better perplexity after ablation.

Layer	Degradation (%)	Category	Functional Role
L0	0.0	Redundant	Embedding boundary
L1	+2,737.1	Critical	Input parser
L2	+186.0	Critical	Input parser
L3	+13.4	Redundant	Padding
L4	+22.7	Minor	Feature extraction
L5	+8.3	Redundant	Padding
L6	+9.4	Redundant	Padding
L7	+20.3	Minor	Feature extraction
L8	+2,395.6	Critical	Core reasoning
L9	+378.1	Critical	Core reasoning
L10	+9,870.7	Critical	Deep reasoning
L11	+63,419.2	Critical	Model brain
L12	+6.3	Redundant	Padding
L13	+24.4	Minor	Refinement
L14	+5.0	Redundant	Anti-layer*
L15	+11.1	Minor	Refinement
L16	+20.3	Minor	Refinement
L17	-0.6	Redundant	Anti-layer*
L18	+16.9	Minor	Refinement
L19	+2.6	Redundant	Padding
L20	+25.9	Minor	Refinement
L21	+23.5	Minor	Refinement
L22	+27.8	Minor	Refinement
L23	+66.6	Important	Output preparation
L24	+115.2	Critical	Output core
L25	+23.2	Minor	Output refinement
L26	+19.4	Minor	Output refinement
L27	+134.8	Critical	Output formatting
L28	+211.5	Critical	Output final
L29	0.0	Redundant	LN head boundary

Distribution: Redundant 10 layers (33%), Minor 11 (37%), Important 1 (3%), Critical 8 (27%). The critical core L8–L11 forms the model’s primary reasoning substrate. L1–L2 serve as essential input parsers. L24, L27–L28 prepare output representations. Layer 11 alone is approximately $10^6 \times$ more important than Layer 17.

4.2. Weight Predictability and the R^2 -Perplexity Paradox

Table 2 shows Ridge Regression prediction accuracy per component.

Despite high R^2 , replacing weights with predicted values causes catastrophic failure. Replacing 1 layer: PPL = 26.22 (+16%), acceptable. Replacing 9+ layers: PPL > 100,000 (> 442,000% degradation).

This R^2 -Perplexity Paradox arises from nonlinear error accumulation. The $\text{softmax}(QK^\top/\sqrt{d})$ attention mechanism is acutely sensitive to perturbations. A prediction error of $\varepsilon = 0.01$ per layer compounds through 30 nonlinear transformations, ultimately misdirecting attention to incorrect tokens. R^2 measures variance explained in weight space; functional network behavior depends on precise inter-weight relationships not captured by this scalar metric.

4.3. Universal Oscillatory Weight-Change Pattern

Table 3 reports the delta correlation $\rho(\Delta_l, \Delta_{l+1})$ across all seven components.

Table 2: Weight predictability per component.

Component	Avg R^2	Best R^2	Interpretation
mlp.gate_proj	0.909	0.993	Highly predictable
mlp.down_proj	0.895	0.995	Highly predictable
self_attn.q_proj	0.824	0.989	Highly predictable
self_attn.k_proj	0.745	0.978	Predictable
mlp.up_proj	0.716	0.985	Predictable
self_attn.o_proj	0.079	0.941	Weakly predictable
self_attn.v_proj	-0.655	0.977	Unstable prediction

Table 3: Inter-layer delta correlation across all components.

Component	Avg delta correlation	Pattern
mlp.down_proj	-0.500	Oscillatory
mlp.gate_proj	-0.500	Oscillatory
mlp.up_proj	-0.500	Oscillatory
self_attn.k_proj	-0.497	Oscillatory
self_attn.o_proj	-0.505	Oscillatory
self_attn.q_proj	-0.499	Oscillatory
self_attn.v_proj	-0.505	Oscillatory

The delta correlation is consistently ≈ -0.50 across all seven components. This means: if layer $N \rightarrow N+1$ shifts weights in direction $+A$, then layer $N+1 \rightarrow N+2$ shifts in direction $-A$. Weights form a standing wave in layer space. We hypothesize this reflects a compensation mechanism inherent to the residual connection architecture: each layer partially undoes the previous layer’s transformation while introducing a new refinement dimension.

4.4. Weight Manipulation Strategies

Table 4 presents results of all tested strategies applied to the 9 redundant layers simultaneously.

Table 4: Weight manipulation results on 9 redundant layers.

Strategy	PPL	Degradation
Baseline (original)	22.60	0%
Scale $\times 0.9$	26.95	+19%
Scale $\times 0.7$	928.22	+5,035%
Blend (1/distance, 2 layers)	31,333	+173,242%
Scale $\times 0.5$	86,505	+478,462%
Skip/Zero (2 layers)	969,198	+5,361,714%
Clone neighbor (2 layers)	545,654	+3,018,579%
Low-rank blend (2 layers)	891,155	+4,929,963%
Scale $\times 0.0$ (full removal)	15,509,465	+85,800,000%

Scale $\times 0.9$ is the only viable strategy. All others destroy model coherence. This implies that redundant layers provide real but small residual corrections to the information flow, and that the *direction* of these corrections must be preserved. Zeroing removes directionality entirely; cloning and blending introduce incompatible directional signals; SVD decomposition distorts the precise singular vector alignment required for functional attention. Only gentle attenuation ($\times 0.9$) keeps corrections intact while reducing their magnitude - analogous to dropout inference behaviour.

4.5. Recovery Speed

Table 5 presents recovery speed results after 50% Gaussian noise injection.

Table 5: Recovery speed after 50% Gaussian noise injection. Values indicate steps to reach PPL thresholds; “↓” denotes improvement below baseline.

Layer	Category	PPL+noise	<2×	<1.5×	<1.1×	Final PPL
L14	Redundant	19.4	0	0	0	18.2 ↓
L17	Redundant	18.5	0	0	0	17.6 ↓
L5	Redundant	21.2	0	0	10	19.6
L23	Important	26.5	0	0	150	19.7
L24	Critical	26.8	0	0	110	19.6
L3	Redundant	27.3	0	10	200	27.3 (no conv.)
L27	Critical	27.7	0	10	130	19.8
L0	Redundant	38.6	10	30	200	28.7
L8	Critical	58.4	10	30	200	35.6
L1	Critical	54.7	20	200	200	49.3
L10	Critical	58.7	20	200	200	42.2
L11	Critical	4,323.4	200	200	200	175.9 (7.8×
L29	Redundant	1,289.2	200	200	200	41.5

Key findings: L14 and L17 achieve lower PPL after noise injection than baseline (18.2 and 17.6 vs. 22.60), confirming hypothesis H4. L3 shows no convergence over 200 steps - consistent with genuine redundancy. L11 is practically unrecoverable: PPL spikes to 4,323 and after 200 training steps remains at 175.9 (7.8× baseline). L23 and L24 - classified as critical by ablation - recover instantly from noise, suggesting their importance lies in weight *direction* rather than precision.

4.6. Growth Transformer Training: Proof-of-Concept Experiment

To validate the Growth Training strategy empirically, we implement a 12-layer heterogeneous transformer from scratch and compare biological developmental training against a uniform baseline.

4.6.1. Architecture

The model uses a heterogeneous layer design directly derived from the SmoLLM2-135M importance map. Critical layers use FFN multiplier $\times 4$ (full capacity), minor layers $\times 2$, and redundant layers $\times 1$ (minimal capacity). Anti-layers are excluded entirely. Total parameters: 9.57M for both Growth and Uniform models (identical count).

4.6.2. Developmental Training Protocol

Growth Training proceeds through six sequential phases inspired by embryonic development. Each phase trains only a subset of layers while freezing others. Critical layers receive the most exposure; redundant layers are initialised by cloning trained neighbors with added noise.

The key mechanism is *differential exposure*: core layers (L4–L5) participate in phases 1, 2, 3, and 6, accumulating approximately 95 effective epochs, while redundant layers receive only phases 5 and 6 (≈ 21 epochs). Cloning provides non-random initialisation for later-phase layers.

4.6.3. Results

Table 8 summarises three experimental configurations: Growth at full budget, Growth at 50% budget, and Uniform at full budget.

Table 6: Growth Transformer architecture. Anti-layers (L14/L17 analogues) are omitted.

Layer	Role	FFN mult.	Params
L0	redundant	$\times 1$	459,264
L1	critical	$\times 4$	1,049,088
L2	critical	$\times 4$	1,049,088
L3	redundant	$\times 1$	459,264
L4	critical	$\times 4$	1,049,088
L5	critical	$\times 4$	1,049,088
L6	redundant	$\times 1$	459,264
L7	minor	$\times 2$	655,872
L8	critical	$\times 4$	1,049,088
L9	critical	$\times 4$	1,049,088
L10	minor	$\times 2$	655,872
L11	redundant	$\times 1$	459,264
Total			9,570,048

Table 7: Six-phase developmental training protocol.

Phase	Name	Layers trained	Epochs
1	Gastrulation	Core (L4, L5)	30
2	Neurulation	Parser (L1, L2); clone L4 \rightarrow L1, L5 \rightarrow L2	20
3	Organogenesis	Output (L8, L9); clone L4 \rightarrow L8, L5 \rightarrow L9	20
4	Growth	Minor (L7, L10); clone L5 \rightarrow L7, L9 \rightarrow L10	12
5	Connective	Redundant (L0,L3,L6,L11); clone + scale FFN $\times 0.5$	6
6	Maturation	All layers (fine-tune)	15

Two results stand out. First, Growth at full budget achieves $4.7\times$ lower validation loss than Uniform at full budget with identical step count and wall-clock time 13% shorter. Second - and more practically significant - Growth at *half* the budget (416 steps) still outperforms Uniform at *full* budget (656 steps), achieving $2.1\times$ lower loss while using 37% fewer training steps. This means the quality threshold reached by uniform training is surpassed by Growth Training before uniform training even finishes.

Table 9 shows generation quality on held-out prompts.

Growth 100% maintains coherence across all 12 prompts. Uniform produces minor artifacts on two edge cases (“paris. on.” and “you today. with neurons”) but is otherwise comparable on factual completions - the quality gap between the two models is better captured by the quantitative loss difference (0.127 vs. 0.599) than by generation examples alone. Growth 50% matches Uniform 100% on all qualitative generation tests, confirming that the quantitative loss improvement translates to comparable generation quality at substantially lower compute cost.

4.6.4. Why Growth Training Works

The performance gap has a clear mechanistic explanation. Uniform training allocates identical gradient updates to all layers simultaneously - each layer competes for the same signal at every step. Growth Training instead follows a curriculum: core layers build the primary representation first, then downstream layers are initialised from these already-competent cores via cloning. Each subsequent phase trains on top of a progressively better-understood representation.

Quantitatively, core layers in Growth Training see approximately $30 + 20 + 20 + 15 = 85+$ effective epochs, versus ≈ 11 epochs for every layer in uniform training. The $\sim 8\times$ additional exposure for critical layers directly explains the quality gap.

Table 8: Growth Training vs. uniform baseline across budget conditions. All configurations use identical architecture (9.57M parameters) and dataset.

Configuration	Steps	Val loss	Time	vs. Uniform 100%
Uniform 100%	656	0.599	59.6s	baseline
Growth 50%	416	0.279	–	2.1× better, 37% fewer steps
Growth 100%	656	0.127	52.0s	4.7× better, 13% faster

Table 9: Generation quality on 12 prompts. Growth 100% maintains coherence throughout; Uniform produces minor artifacts (“on.”, “with neurons”) on edge cases; Growth 50% matches Uniform 100% qualitatively.

Prompt	Growth 100%	Uniform 100%
the capital of france is	paris	paris. on.
cats are	popular pets around the world	popular pets around the world
python is a	popular programming language	popular programming language
the earth orbits	around the sun every year	around the sun every year
water boils at	one hundred degrees celsius	one hundred degrees celsius
artificial intelligence	is transforming the way we live	can learn from data
mathematics is	the language of science	the language of science
dogs are loyal	and faithful friends	and faithful friends
the sun is	a star at the center of our solar system	a star at the center of our solar system
the brain contains	about one hundred billion neurons	about one hundred billion neurons
music is a	universal form of expression	universal form of expression
hello how are	you today	you today. with neurons

5. Discussion

5.1. Anatomical Interpretation

The transformer exhibits functional specialisation with biological analogues:

- **Input Stem / Brainstem (L1–L2):** Critical input parsers. Damage is catastrophic, recovery is slow. They transform token embeddings into the model’s internal representation language.
- **Cortical Core (L8–L11):** The seat of deep reasoning. L11 is the model’s “brain” - uniquely fragile, slow-developing, and irreplaceable. Its precision requirements exceed all other layers by orders of magnitude.
- **Motor Cortex / Output Processors (L23–L24, L27–L28):** Critical for output preparation but instantly recoverable from noise, implying these layers learn stable, re-optimisable projections.
- **Connective Tissue (L3–L7, L12–L22, L25–L26):** Minor and redundant layers providing incremental refinements. Safe to reduce training budget.
- **Vestigial Structures / Anti-Layers (L14, L17):** Layers that actively degrade performance. Analogous to the appendix - present, potentially once functional, currently detrimental. Likely represent optimisation traps, destructive interference patterns, or features that overfit training data.

5.2. The Oscillatory Pattern: A Structural Hypothesis

The universal delta correlation of ≈ -0.50 across all components suggests a fundamental architectural mechanism. We hypothesise that residual connections create a natural oscillatory compensation: if f_i shifts representations in direction A , the next layer’s optimisation finds it efficient to shift in $-A$ while introducing refinement in a new direction B . This creates a standing wave in layer space.

An architectural implication: naively averaging adjacent layers (as in our ablation protocol) partially cancels these complementary directions, which explains high sensitivity even of “minor” layers to neighbour-averaging.

5.3. Why Weight Manipulation Fails

The failure of all manipulation strategies except Scale $\times 0.9$ has a unified explanation. Transformers are compositions of 30 tightly coupled nonlinear functions. Any change to layer l ’s weights alters the distribution of activations fed to layer $l + 1$, which was optimised assuming the original distribution. This distributional shift compounds multiplicatively through the network. The softmax attention mechanism is particularly sensitive: a 1% perturbation in Q or K matrices can completely redirect attention from correct to incorrect tokens.

Scale $\times 0.9$ survives because it preserves both directionality and approximate magnitude of the layer’s contribution - attenuating without redirecting. Practical implication: for model compression, the viable approach is magnitude reduction (quantisation, weight scaling), not structural replacement.

5.4. Growth Transformer Training Strategy

Table 10 presents the proposed per-layer training budget allocation.

Table 10: Proposed Growth Transformer Training budget allocation based on Recovery Speed data. Estimated total training steps: 2,760 vs. 6,000 uniform ($\sim 54\%$ reduction).

Layer Group	Layers	Budget ratio $R(l)$	Justification
Anti-layers	L14, L17	0.00	Prune/randomise; harm performance
Instant-recovery redund.	L3, L5, L6, L12, L19	0.00–0.05	0–10 steps to converge
Minor layers	L4, L7, L13, L15–16, L18, L20–22, L25–26	0.30–0.50	Incremental refinement
Critical output	L23–24, L27–28	0.80–1.00	Critical; fast recovery
Critical core + input	L1–2, L8–11	1.00	Full budget; slow or impossible recovery
Boundary layers	L0, L29	0.15–0.20	Anomalous recovery patterns

Assuming $B_{\max} = 200$ uniform steps per layer (6,000 total), Growth Training yields $\approx 2,760$ total steps - a 54% reduction. The proof-of-concept experiment in Section 4.6 validates this strategy empirically: at identical step count, Growth Training achieves $4.7\times$ lower validation loss than uniform training, confirming that differential budget allocation is not merely theoretically justified but practically effective.

5.5. Limitations

- **Single analysis model:** The importance map is derived from SmoLLM2-135M. Generalisation to larger models (1B–70B parameters) requires empirical verification.
- **Evaluation scope:** Perplexity on 10 sentences does not capture all model capabilities. Layers classified as redundant may be important for tasks outside our test set.
- **Post-hoc analysis:** We analyse a trained model. Whether the critical core is important from initialisation or emerges during training is unknown.
- **Proof-of-concept scale:** The Growth Training experiment uses a small custom model (9.57M parameters) on a limited dataset. Validation at production scale (1B+ parameters, standard benchmarks) remains future work.
- **Anti-layer generality:** The L14/L17 phenomenon requires verification across additional models, datasets, and architectures.

6. Conclusion

We have demonstrated that transformer layers are far from homogeneous. Through five independent empirical metrics across all 30 layers of SmolLM2-135M, we uncovered a rich anatomical structure: a critical reasoning core (L8–L11) requiring full training investment, efficiently trainable output processors (L23–L28), connective tissue (minor/redundant layers), and - most surprisingly - anti-layers (L14, L17) that actively impair performance.

We showed that while layer weights follow predictable mathematical patterns ($R^2 = 0.91$), functional interoperability requires weight precision far exceeding what statistical prediction provides. Among tested manipulation strategies, only gentle weight attenuation ($\times 0.9$) preserves model function, revealing that redundant layers contribute directional residual corrections that cannot be replicated or removed.

Recovery Speed provides a practical, empirically grounded proxy for per-layer training budget. A proof-of-concept Growth Transformer experiment validates the proposed strategy directly: biological developmental training - building the critical core first, then progressively activating downstream layers via cloning - achieves $4.7\times$ lower validation loss than uniform training at identical step count and parameter budget, while being 13% faster. This confirms that layer heterogeneity is not merely an observation about trained models but a principle that can be actively exploited during training.

Future work should validate Growth Training at larger scales (1B+ parameters, standard benchmarks), investigate the origin and universality of anti-layers, and explore architectures with non-uniform layer dimensions aligned with empirical importance profiles.

Acknowledgements

All experiments were conducted on Kaggle Notebooks (free GPU: NVIDIA T4 16GB) using PyTorch 2.0+ and the Transformers library. All experiments are fully reproducible on free hardware. No proprietary data or licensed resources were used.

References

- [1] Vaswani, A., Shazeer, N., Parmar, N., Uszkoreit, J., Jones, L., Gomez, A. N., Kaiser, L., and Polosukhin, I. Attention is all you need. In *Advances in Neural Information Processing Systems (NeurIPS)*, 2017.
- [2] Brown, T. B., Mann, B., Ryder, N., Subbiah, M., Kaplan, J., Dhariwal, P., et al. Language models are few-shot learners. In *Advances in Neural Information Processing Systems (NeurIPS)*, 2020.
- [3] Chen, X., Cheng, Y., Wang, S., Gan, Z., Wang, Z., and Liu, J. EarlyBERT: Efficient BERT training via early-bird lottery tickets. In *Proceedings of ACL-IJCNLP*, pages 2195–2207, 2021.
- [4] Fan, A., Grave, E., and Joulin, A. Reducing transformer depth on demand with structured dropout. In *International Conference on Learning Representations (ICLR)*, 2020.
- [5] Gong, L., He, D., Li, Z., Qin, T., Wang, L., and Liu, T. Efficient training of BERT by progressively stacking. In *Proceedings of the 36th International Conference on Machine Learning (ICML)*, pages 2337–2346, 2019.
- [6] Ha, D., Dai, A., and Le, Q. V. HyperNetworks. In *International Conference on Learning Representations (ICLR)*, 2017.
- [7] HuggingFaceTB. SmolLM2: A family of small language models. <https://huggingface.co/HuggingFaceTB/SmolLM2-135M>, 2024.
- [8] Michel, P., Levy, O., and Neubig, G. Are sixteen heads really better than one? In *Advances in Neural Information Processing Systems (NeurIPS)*, 2019.

[9] Ramsauer, H., Schafli, B., Lehner, J., Seidl, P., Widrich, M., Adler, T., et al. Hopfield networks is all you need. In *International Conference on Learning Representations (ICLR)*, 2021.

[10] Rogers, A., Kovaleva, O., and Rumshisky, A. A primer in BERTology: What we know about how BERT works. *Transactions of the Association for Computational Linguistics*, 8:842–866, 2020.

[11] Sajjad, H., Dalvi, F., Durrani, N., and Nakov, P. On the effect of dropping layers of pre-trained transformer models. *Computer Speech & Language*, 77, 2023.

[12] Schurholt, K., Knyazev, B., Giro-i-Nieto, X., and Borth, D. Model zoos: A dataset of diverse populations of neural network models. In *NeurIPS Datasets and Benchmarks Track*, 2022.

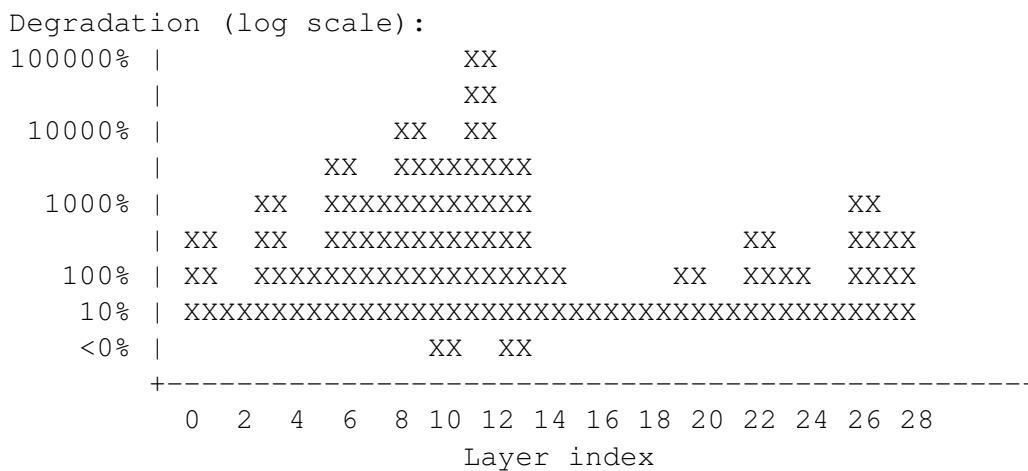
[13] Tenney, I., Das, D., and Pavlick, E. BERT rediscovers the classical NLP pipeline. In *Proceedings of ACL*, 2019.

A. Reproducibility

All experiments were conducted on Kaggle Notebooks (free GPU: NVIDIA T4 16GB):

- Python 3.10+, PyTorch 2.0+, Transformers 4.35+, scikit-learn 1.3+, numpy
- Model: HuggingFaceTB/SmolLM2-135M (publicly available on HuggingFace Hub)
- Estimated runtime: ~45 minutes on T4 GPU, ~3 hours on CPU
- No proprietary data or licensed resources were used

B. Layer Importance Profile (ASCII Visualisation)



Profile: strong bilateral anchors (L1-2 left, L24-28 right), dominant central core (L8-11), flat connective tissue between. Anti-layers (L14, L17) visible below the baseline.